IEEE Robotics and Automation Letters (RA-L) paper, presented at ICRA 2024, Yokohama, Japan. Cite as RA-L paper.

Learning-Based Object Recognition via a Eutectogel Electronic Skin Enabled Soft Robotic Gripper

Mo Deng, Fengya Fan, and Xi Wei

***Abstract*—Compared to the traditional robot, which is rigidly structured, the soft robot, usually made of soft material, or following a continuous movement pattern, has attracted extensive attention due to its unique features, such as high adaptivity to various unstructured environments and safe interaction with living beings through the deformable interface. However, mechanical and morphological requirements limit the design and implementation of a compatible sensing module, which restricts the further development of robotic functionality. Here, we designed a flexible soft sensing Wire with the piezoresistive Eutectogel packed in an Ecoflex tube (WEE), which is sensitive, stable, and easily manipulated. The wire and its array facilitated the perception function of the soft gripper and acted as the Electronic skin (E-skin) to acquire information from grasped objects. With the built-in E-skin, the gripper achieved object recognition at an accuracy of 93.78% for standard geometric objects in 9 categories based on a machine learning model. In addition, our design successfully demonstrated its application in fruit sorting, which proves its robustness and versatility. The proposed WEE-based E-skin can be easily applied to other soft robots with facile integration and further expedites advanced functionalization in robot-object interaction.**

***Index Terms*—Soft robot applications, soft sensors and actuators, modeling, control, learning for soft robots, E-skin, soft gripper.**

I. Introduction

CLASSICAL robots commonly follow the articulated design to control the precision in the movement, although stable, but rigid and hard to adapt to the change of interaction objects. Soft robots, made of soft material or following a continuous movement pattern [1], have attracted researchers' attention over the past few years. Based on their material/structure nature, soft robots own unique features such as dynamic environmental adaptability, profound degrees of freedom in morphological deformation, and safe interaction with living beings through energy absorptive interface [2], [3], [4], [5]. Taking the soft robot gripper as an example (also as the soft robot model discussed and studied in this work), one model configuration can apply in dynamic grasping tasks for objects with diverse shapes and stiffness through self-adapting due to the excellent deformation tolerance on the contacting interface [6], [7]. This cannot be fulfilled by rigid robots often designed for structured environments without compatible adapters. For example, rigid robots need to change the configuration of components [8], or even replace them [9], in order to meet the requirements of different tasks. However, the challenge of closed-loop control of the soft robot remains unsolved. Perception is a critical element of the closed-loop control body [10], [11], [12] as it provides the signal feedback linked to the robotic motion as well as the interaction between the soft robot and the objects, which can be translated and applied in object recognition and other advanced functionality design.

A common approach for developing suitable sensing modules is to form an array of simple, flexible tensile sensors to simulate the skin's nervous system to detect surface stimuli, usually referred to as "electronic skin" (E-skin) [13]. Many designs have been studied and proven effective in detecting the pressure signal and achieving higher accuracy by identifying tangential force and normal force [14], or realize the multimodal measurement of the magnetic field, temperature, and other parameters [15], or realizing dynamically reconfigurable and damage resistant thermal, tactile information detection [16], and tactile recognition by integrating sensors on gloves [17], etc. However, most reported sensor units/arrays are often expensive, difficult to fabricate, and hard to implement when changing scale.

An alternative approach is to mix/fill conductive materials in elastomers as the sensing module of the gripper, such as carbon nanotubes modified polydimethylsiloxane to construct the E-skin, in which the physical deformation signal of the sensing unit is translated to electrical signal [18], [19] But the elasticity of this material is inconsistent with that of the soft gripper, which leads to the displacement between the sensing module and the grasping interface. Another widely used E-skin material is a liquid metal, which can be embedded in the soft gripper during fabrication [20], [21]. The change in its resistance correlates to the interaction signal on the soft gripper. However, it is commonly observed that the liquid metal embedding channel disconnects if the degree of deformation is high. Although designing microchannels to pattern liquid metal could mitigate this problem [22], [23], this method significantly increases the manufacturing complexity and cost. There are also sensing methods with optical sensors, such as optical waveguides [24] and optical fibers [25]. However, optical sensors usually require light sources and optical detectors, which is difficult to implement. Computer vision with recurrent neural networks can also enable E-skin's performance in the soft robot perception [26], but the cost of the camera is expensive, and the field of view of

Manuscript received 30 April 2023; accepted 1 September 2023. Date of publication 15 September 2023; date of current version 4 October 2023. This letter was recommended for publication by Associate Editor D. Shin and Editor C. Laschi upon evaluation of the reviewers' comments. This work was supported in part by USTC Start-up Grant under Grant KY0110000033 and in part by the Natural Science Foundation of Anhui Province, Young Scholars under Grant BJ2060000039. *(Corresponding author: Xi Wei.)*

Mo Deng and Fengya Fan are with the Department of Computer Science and Technology, University of Science and Technology of China, Hefei, Anhui 230026, China (e-mail: sa2001167@mail.ustc.edu.cn; fanfengya@mail.ustc.edu.cn).

Xi Wei is with the Department of Chemistry, University of Science and Technology of China, Hefei, Anhui 230026, China (e-mail: wxi@ustc.edu.cn).

Addtional experiment data is avaiable on https://github.com/DengMo0909/Experimental-data

Digital Object Identifier 10.1109/LRA.2023.3316096

IEEE Robotics and Automation Letters (RA-L) paper, presented at ICRA 2024, Yokohama, Japan. Cite as RA-L paper.

the camera needs to stay clear without any blockage during the motion. Therefore, there is substantial demand for a new E-skin design that is elastically compatible, easy to integrate, low cost, and facile to operate while remaining sensitive to perception.

Conductive gel, a soft material in which the distribution of internal ions changes with its mechanic deformation, presents piezoresistive features. Its tunable resistivity, flexibility, stiffness, and biocompatibility make it a suitable E-skin substrate for a soft gripper. A variety of flexible strain and pressure sensors has been developed [27], [28] and demonstrated their applications in soft grippers and wearable devices [29] to perceive proprioceptive motion [30] or object recognition [31]. However, the following problems limit its further development as E-skin in soft robots: 1) many conductive gels are hydrogels, and the performance is often compromised by water evaporation during testing [32]; 2) it is difficult to mount the soft gels stably on the surface of soft grippers due to weak interface adhesion and high deformation degree during motion [33]; 3) the soft texture makes it prone to fracture when directly in contact with sharp objects [34], 4) the molding and implementation process of the sensing units is often cumbersome, Moreover, there can be associated risks, such as the toxicity commonly found in ion gels [35].To address the abovementioned challenges, eutectogel is a viable option for soft strain and tensile sensors: its tunable softness and elasticity are similar to other conductive gels, but its conductivity relies on the deep eutectic solvent (DES) instead of a water-based system or ionic liquid. DES is a eutectic mixture in which the melting point is significantly lower than the melting points of the individual pure substances. Some DESs possess the basic properties of ionic liquids. These features, of the eutectogel produced with DES, improves its service life since less evaporation issue; compared to other non-water based gels, such as ionic gels, the preparation of eutectogel is simpler, cheaper, greener, and with low toxicity [36]. In this work, we fabricated the wire-shaped sensors by packing the eutectogel with hollow ecoflex tubes. Since our gripper was made of ecoflex, the ecoflex sheath of the sensors allowed them to be securely embedded and mounted on the surface of the soft gripper. In addition, the layer of ecoflex protected the eutectogel away from fracture when in direct contact with sharp objects. This fabrication method is simple and tunable, which facilitates ready to use sensors with increased homogeneity and shelf life. The proposed design effectively addresses the aforementioned issues.

In addition, manufacturing and control strategies are important in developing soft robotics. In this work, we chose to use the 3D printing technique for quick prototyping [37] and the finite element simulation (FEM) method to optimize our gripper model. In terms of control strategy, for simplicity, effectiveness, and ease of operation, we adopted a fluid-driven open-loop control mode [38]. This control strategy is relatively straightforward and facilitates rapid research in perception.

In this work, we developed a soft pneumatic gripper with a built-in eutectogel-based E-skin to achieve object recognition through grasping. To achieve facile implementation, we established a method to fabricate a wire-shape strain and tactile sensing unit by packing eutectogel into hollow ecoflex tubes (WEE) and embedding the sensing wire closely under the grasping contact surface of the silicone soft gripper during the molding process. With this strategy, the E-skin constituted of the sensing units can be well-positioned inside the gripper without any adhesion layer while remaining sensitive and secured. The gripper only requires a portable air pump to operate and can identify

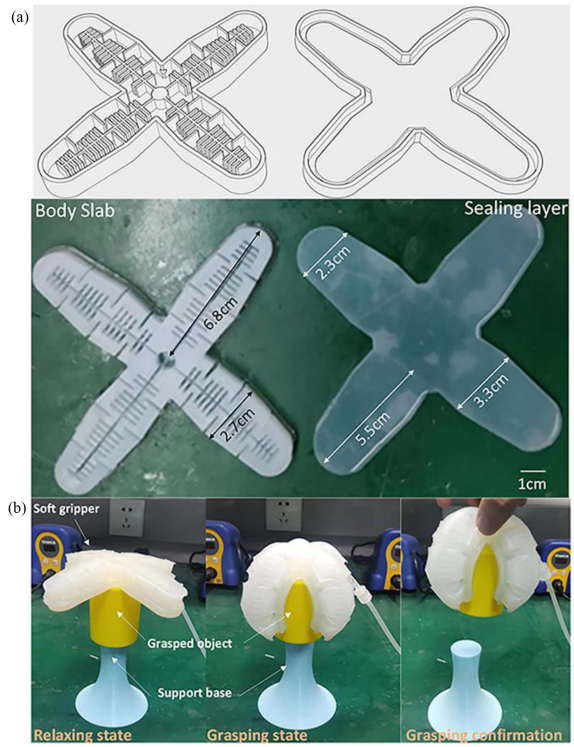

Fig. 1. (a) 3D modeling schematic of the mold used to fabricate the soft gripper (top) and the casted gripper parts with ecoflex (bottom). (b) Representations of the pneumatic gripper motion: Pre-grasping, grasping, and grasping to lift. The maximum bending angle of the air arm can reach $> 83°$. The yellow cylinder shown as the grasped object is 4.5 cm in diameter and 5.5 in height.

grasped objects through the electrical signal collected from the E-skin. The machine learning method was used to create a multilayer perception (MLP) model to learn the electrical signal changes recorded in the E-skin during the grasping process and identify the grasped objects based on their geometrical shape at an accuracy of 93.78%. Moreover, it was observed that the recognition accuracy could be greatly improved by grasping data from multiple angles instead of one, indicating that scaling up the sensing units can further advance the E-skin's performance when more feature data is required from the objects. At last, the soft gripper equipped with eutectogel E-skin was applied in fruit recognition and successfully classified 6 types of fruits with a 93.89% accuracy, which shows its potential in applications such as automatic sorting/packing for fruit or other similar fresh products with similar geometric features in factories or supermarkets.

II. Design and Fabrication of the Softer Gripper With E-skin

A. Fabrication of the Soft Gripper

In this work, we designed the soft gripper using a classical pneumatic soft gripper model: a four-arm gripper with an air chamber to control the grasping motion by inflation/deflation [39]. We modified the internal air chamber structure to optimize the arm bending angle during inflation to improve its air pressure response. The gripper body slab with pneumatic chamber and the sealing layer was cast in 3D printed molds with Ecoflex^{TM} 00-10 (Fig. 1(a)). In order to reserve the socket for the inflatable

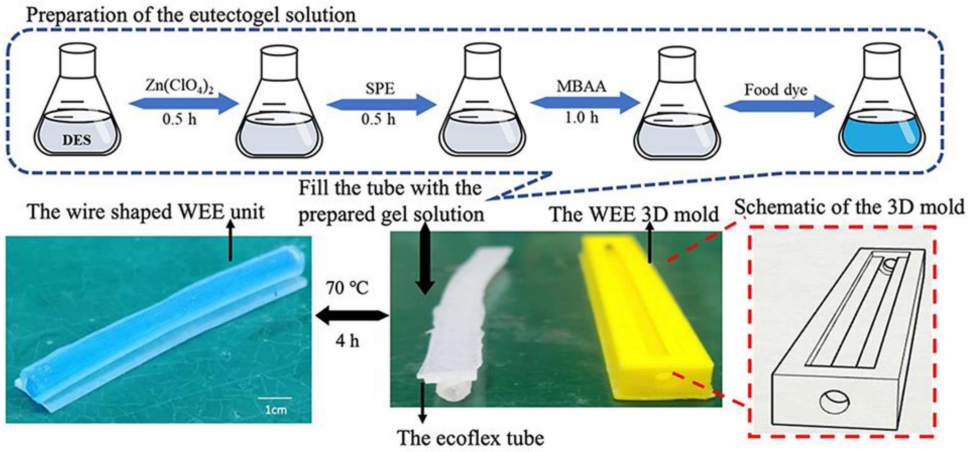

Fig. 2. Fabrication process of the wire-shape sensing unit by packing eutectogel into hollow ecoflex tubes (WEE). The ecoflex tube was cast and released from a 3D-printed mold together with a steel tube. The eutectogel solution was injected into the ecoflex tube for gelation to form a basic WEE unit.

TABLE I
TENSILE STRESS-STRAIN OF ECOFLEX AND WEE UNIT

Tensile stress-strain	Stress	
	Ecoflex 00-10	*WEE UNIT*
Stretch 50%	30kPa	16 kPa
Stretch 100%	50 kPa	20 kPa
Stretch 150%	90 kPa	35 kPa
Stretch 200%	140 kPa	68 kPa

TABLE II
THE DIMENSIONS OF THE GEOMETRIC OBJECTS USED IN THE EXPERIMENT

Cubic (big):	60*60*100 (l*w*h)	**Cylinder (big):**	30*100 (r*h)
Cubic (small):	40*40*50 (l*w*h)	**Cylinder (small):**	45*50 (r*h)
Cubic (long):	80*40*20 (l*w*h)	**Ball (big):**	40 (r)
Ball (small):	30 (r)		

Note: l: length; w: width; h: height; r: radius. (Unit: mm).

rubber hose, a smooth metal tube of appropriate size was inserted in the mold prior to casting and pulled out after the ecoflex was cured. A layer of Sil-Poxy^{TM} adhesive was applied on the side of the hollow rubber hose and the $\sim$ 6mm thick sealing layer. The body slab and the sealing layer were assembled and glued together with the rubber hose placed into the socket. The completed gripper was tested, and verified its functionality by inflating air to control the grasp motion (Fig. 1(b)).

B. Design and Realization of E-Skin Wire Sensing Unit

We followed a previously reported protocol to prepare the eutectogel: ternary DES composed of low-cost choline chloride (ChCl), ethylene glycol (EG), and urea with a stoichiometric ratio of 1:2:1 was mixed as the solvents [40]. To prepare 2ml eutectogel, we used 2ml DES, 1.4895g $Zn(ClO_4)_2$0.6321g 3-((2-(methacryloyloxy)ethyl)dimethylammonio)propane-1-sulfonate (SPE) and 0.006g N, N'-methylene bisacrylamide (MBAA) by following the procedure as shown in Fig. 2.

We adjusted the proportion for zwitterionic monomers SPE to increase tensile strength to make the eutectogel suitable as electronic skin for repeated stretches during sensing. The weight of the prepared gel was almost the same after 25 days at room temperature. The maximum strain was more than 200% proving good mechanical properties.

To reduce batch variation and facilitate easy handling, the eutectogel was prepared and injected into a pre-fabricated ecoflex hollow tube to solidify in wire shape WEE (Fig. 2). Due to the inherent adhesive nature, the eutectogel core can be well attached to the ecoflex shell and can respond to shell deformation. Table I shows the tensile stress-strain data of the WEE unit and ecoflex, indicating that the shell deformation (as the gripper motion) range is not limited by the core structure. The piezoresistivity-strain tests of the WEE unit (4mm in diameter, 11.5 cm in length) are shown in Fig. 3. The test data demonstrated that our fabricated sensor could accurately perceive the differences in sensor deformation (stretching), contact force magnitude, and force contact location, which was reflected in the real-time current signal. Therefore, we believe this sensor can be used for constructing E-skin and applied to object classification in subsequent experiments. The WEE unit is simple to manipulate by molding and then cutting into fragments with the desired size. The structure of the shell is not only to protect and pack sensing material but also serves as a bonding interface to the soft gripper made of the same material.

C. E-Skin Integration

The WEE units were placed closely under the grasp contact surface of the soft gripper in each arm to serve as the E-skin. When casting the sealing layer, the WEE units were positioned in the mold refilled with about 3mm-thick uncured ecoflex. After cured, another 3mm thick ecoflex was poured to fill the mold and cured to complete the sealing layer with semi-embedded sensors. The position was selected in the sealing layer to ensure: 1) the air chamber was not affected, 2) no additional structure extruding on the grasp interfaces, and 3) the grasped object could be sensitively detected. In addition, considering the width of the air arm, we decided to use two parallel WEE units embedded in each arm to serve as one data-collecting channel, as shown in Fig. 4. Each pneumatic arm was equipped with two parallel WEE units mainly for the following reasons: to enhance the

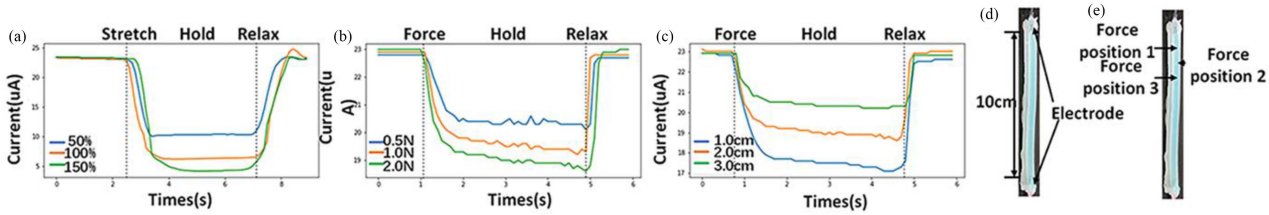

Fig. 3. Piezoresistivity-strain test of a 10 cm WEE unit with 2 V voltage applied across the electrodes. (a) The current response in the WEE unit when stretched at 50%, 100%, and 150%. (b) The current response in the WEE unit when 0.5 N, 1 N, and 2 N forces were applied in the position ∼2 cm away from one side of the WEE unit. (c) The current response in the WEE unit when 2N forces were applied in the position ∼1 cm, 2 cm, and 3 cm away from one side of the WEE unit. (d) The WEE unit schematic diagram for experiments, indicating the positions of the electrodes. (e) The positions of forces in C are marked, with a spacing of 1cm.

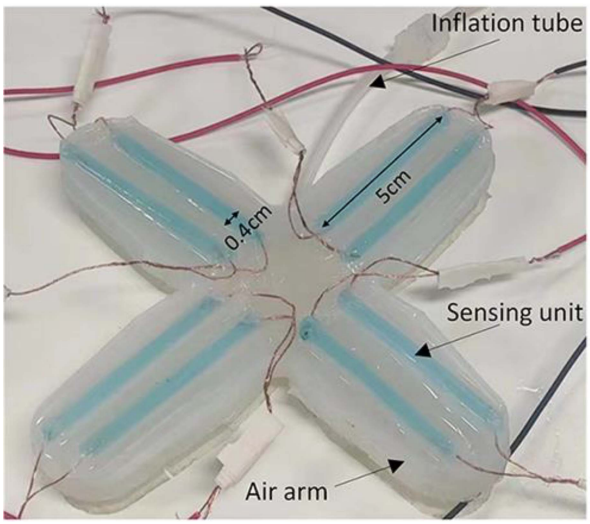

Fig. 4. Soft gripper integrated with the E-skin with 2 parallel WEE units in each arm as one data collection channel.

current magnitude: by using two parallel WEE units, the current value can be doubled maximumly; and to provide better sensing stability for grasping objects, by increasing the sensing area to ensure a more secured contact signal collection than the single unit design. Upon completing the E-skin integration, the soft gripper can perceive its own motion by sensing the bending angle and the grasped objects by judging the size, shape, and other geometrical parameters.

III. Experimental Setup and Data Acquisition

A. Experimental Setup

To set up a consistent experiment condition and minimize manual interference, we set the soft gripper in a fixed position to grasp the objects from the top surface. Although it was proved that the soft gripper could stably grasp all the objects used in the experiment and lift them, we did not include weight as a study parameter in this work but focused on geometrical information. Thus, grasping was defined as a tight contact of the air arms wrapping around the objects but not lifting objects in the air. We optimized the inflating air volume as 110 mL injected from a syringe to grasp all the objects (Fig. 1(b)). In total, we used 7 standard objects with 9 labels for the grasping experiment, among which each cylinder object was considered as 2 types of testing scenarios depending on the "lying" position or "standing" position marked as 0 and 1, correspondingly.

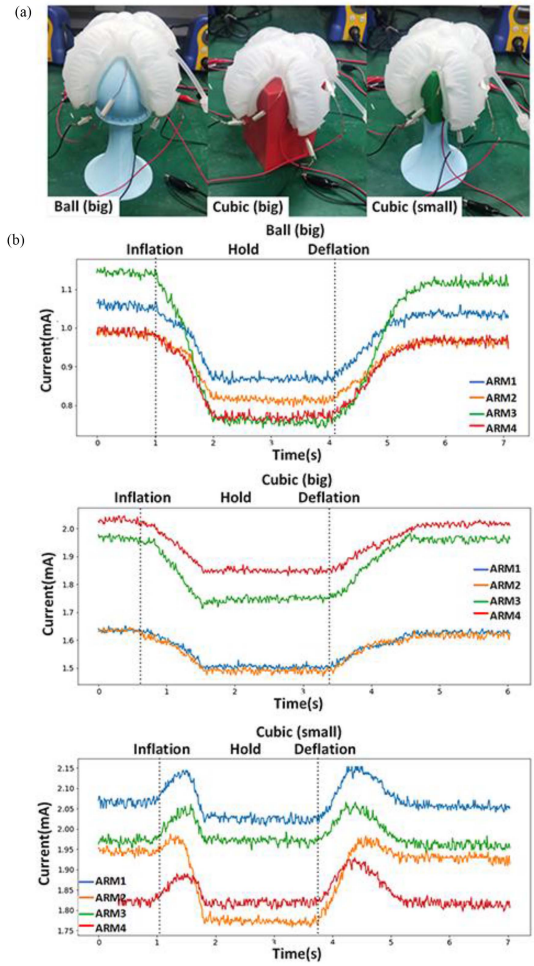

Fig. 5. (a) The experiment set-up for objects grasping with the soft gripper integrated with E-skin. Objects are shown in the picture: Ball (big), cubic (big), and cubic (small). (b) Time series data of the current response was collected from E-skin in the gripper arms. Significant differences among groups with different grasping objects can be observed. For the group with the same object, although there were variations in the baseline among the channels, more identical features were shared within the group.

B. Data Acquisition

The soft gripper was inflated to grasp objects and held in position for ∼2s before deflation. 2V voltage was applied to E-skin to monitor the piezoresistive response. The data collected during the inflation-hold-deflation process was recorded by the 8-channel analog input module (Beckhoff EL3048) at a sampling frequency 100 Hz with a programmable logic controller

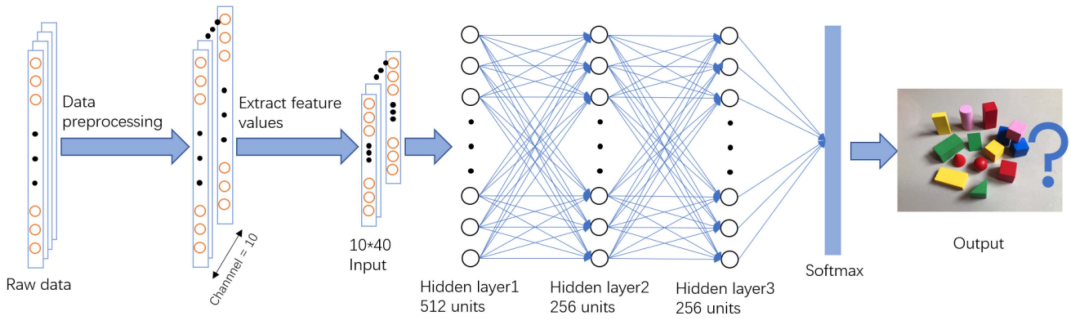

Fig. 6. Schematic of the MLP neural network architecture. Each hidden layer has a drop layer with a loss probability of 0.5 to prevent overfitting. The activation function for hidden layers uses rectified linear unit (ReLu).

(PLC) program in the software of Twincat. Fig. 5 shows representative current time-series data collected from each sensing unit from the grasping process of 3 objects. These data were used in the subsequent training and testing of the MLP model after preprocessing. From Fig. 5, it was observed that there were significant differences in the signal responses of the sensors to the objects with different shapes through grasping. These signal shifts compared to the baseline were utilized to distinguish the geometric features of the testing objects. The reason for the variations in the baseline measurements in Fig. 5(b) could be caused by the manual fabrication batch variation and positioning difference during the embedding process. However, these variations did not affect the object recognition process in our subsequent experiments since the signal shift to the baseline represented the feature information not the absolute value.

C. MLP Training

The recorded grasping process followed the symmetric inflation-hold-deflation process, with around ∼600 output data points. To focus on the signal change analysis, the slope of every 5 data points away from the center point within a 50 data points radius and 25 data points for the rest was calculated and filtered with scipy lowpass. A total of 40 slope values were generated as the dataset of one arm and 4 datasets for each grasping experiment with the E-skin. To increase the dataset, 6 more artificial datasets were generated by subtracting the 4 direct experiment datasets from each other. A total of 10 datasets with 40 values in each were obtained for one grasping experiment, 9 objects were tested, and each was repeated 210 times.

We implemented the MLP with three hidden layers as the model for training. The structure of the model is shown in Fig. 6. The input layer corresponded to 10 datasets with 400 characteristic values as the input at one time. After that, three hidden full connection layers were designed, corresponding to 512256256 hidden units. Each full connection layer was followed by a drop layer with a loss probability 0.5 to avoid over-fitting. The output layer provides 9 outputs corresponding to 9 labels from 7 objects.

IV. Experimental Results

A. Object Grasping Recognition

To evaluate the performance of the E-skin in object recognition, we selected 7 objects of 9 varied shapes, sizes, and positions in the grasping experiments (Fig. 7(a) and (b) and Section III-A). The specific dimensions of the object are listed in Table II. The deformation on the gripper-object interface resulting from the grasping motion can be recorded by the E-skin with WEE units. 400 values were collected from one grasping experiment, objects with 9 labels were tested, and each was repeated 210 times. 160 datasets from the objects with every label were applied to training, and the rest was used for testing by random selection. Fig. 7(c) shows the recognition accuracy of the MLP model, with an overall recognition accuracy of 85.6%. Among them, the cubic (small) cannot be easily differentiated from the result of the cylinder (small)1.

In the process of grasping, the approaching angle was fixed. The main information the E-skin can acquire is the soft gripper arm bending angle against the object and the interface deformation on the contact position. In each arm, there were 2 WEE units installed parallelly to provide feedback as one channel. When grasping cylinder (big)1 and cubic (big), although they were similar in size, which means the bending angle of the gripper was roughly the same, the difference between the two objects can still be captured by sufficient data collected from the contact area that usually crossed both units. For smaller objects, the contact area was narrower, resulting in the loss of efficient contact: this could be why E-skin cannot precisely capture the geometrical information.

To verify this assumption, we changed the grasping approach from fixed positions to random multi-angle grasping for cubic (small) and cylinder (small)1 and tested again 210 times. Exception for the change in the contact angle, the rest follow the same protocol for grasping, data processing, and model training. Fig. 7(d) shows the recognition accuracy of the model for 9 types of objects after supplementing this data set, which can reach 93.78% of recognition accuracy. This proves that our model is effective in recognition accuracy and that random angle grasping is helpful in obtaining sufficient geometrical features when the size of objects is limited. This indicates that the recognition accuracy of our gripper can be enhanced when objects are placed at random angles.

B. Geometry Recognition With Increased WEE Units

It is self-explanatory that the arrayed sensing system trends commonly feature miniaturized unit sizes and high sensor density. A moderate, low-cost, and facile design that provides sufficient information about interacting objects yet still holds the potential for high resolution is important for practical purposes. Here we explored the potential of the proposed E-skin by fabricating a half-size WEE unit to embed in the air arm and doubling the number of channels of the E-skin, as shown in Fig. 8(a). The

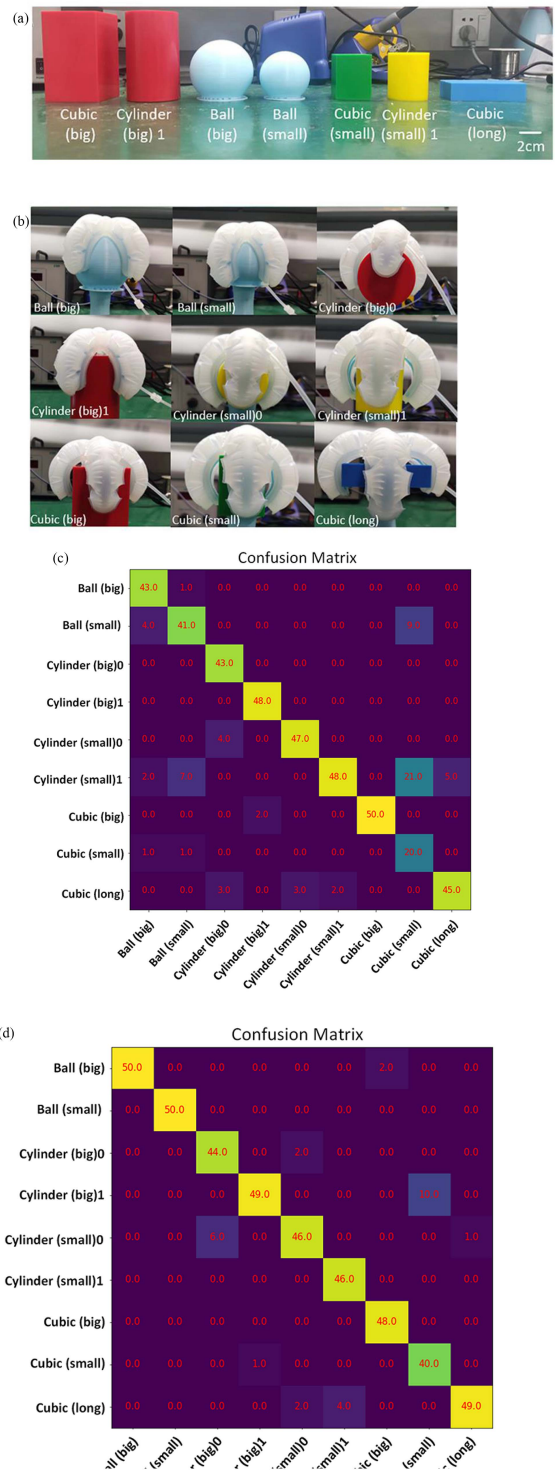

Fig. 7. (a) 7 objects were used in the grasping experiment. In total, 7 objects with 9 labels were used to form 9 individual experiment groups. (b) The grasping postures corresponding to each label. Classification test confusion matrix with datasets from (c) experiments with grasping from a fixed position and (d) experiments with grasping from a randomly selected angle. The confusion matrix for the classification test consists of 450 groups of test datasets. Each row and each column represent an instance in the predicted class and the actual class, respectively. The values on the diagonal represent the correct results. The color represents the number of instances where the object with the corresponding vertical coordinate is recognized as the category of the corresponding horizontal coordinate. The closer the color is to yellow, the higher the recognition rate.

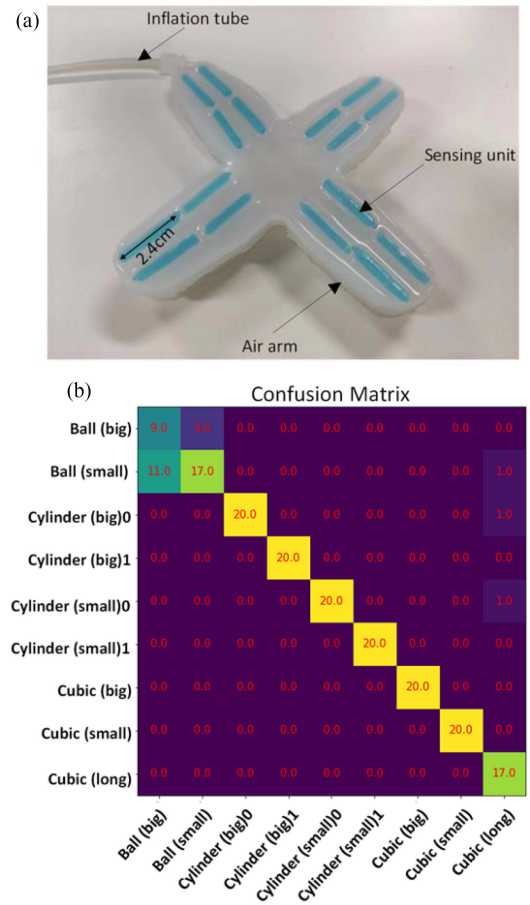

Fig. 8. (a) The image of the soft gripper with E-skin of half-size WEE units and 8 channels in total. (b) Classification test confusion matrix with datasets from experiments with the gripper showing in (a) at a fixed position. The confusion matrix consists of 180 groups of test datasets with other specifications similar to those in Fig. 7.

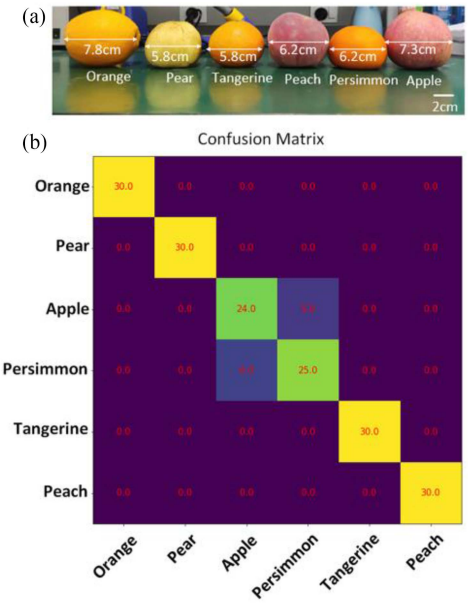

Fig. 9. (a) 6 types of fruits used in the experiments. (b) Classification test confusion matrix with datasets from fruit grasping experiments with the E-skin equipped soft gripper. The confusion matrix consists of 180 groups of test datasets, with other specifications similar to those in Fig. 7.

gripper with this version of E-skin was tested to evaluate its performance by using 9 types of geometrically labeled objects used previously. 50 times grasp on each type was performed to build datasets, among which 30 were randomly selected for training and the rest 20 for testing. The results are shown in Fig. 8(b). Interestingly, the MLP model can recognize different objects with high accuracy for objects with discontinuity surfaces, even though the data size is greatly reduced. For objects with surfaces of continuity (such as ball-shaped), the recognition effect is poor.

One obvious change that resulted from reducing the WEE unit and increasing the units' number is that the spatial resolution was increased at the cost of decreased signal magnitude. This could explain why the recognition accuracy for objects with discontinuity surfaces improved, but the rest did not. The deformation on the interface caused by the contact on the vertices or the edges of cylinders and cubes can be sensed more efficiently due to the higher sensing unit number per area. Although the datasets used for the study are smaller in this version, they provided more geometrical information, and consequently, the MLP model showed improved effectiveness in testing than before. For balls, the feature is homogenous; thus, the gripper with this version of design mostly recognizes objects by accessing its size information based on the gripper arm bending angle, and naturally, its recognition accuracy declined with smaller datasets. These results indicate the versatility of the E-skin design and its compatible configurations for objects with different features. With a sufficient dataset, the E-skin with higher arrayed WEE units works better than those with lower units. When the dataset is limited, the same design can still offer improved performance when grasping objects with discontinuity surfaces.

C. Application in Fruit Recognition

In supermarkets, fruit farms, or assembly lines in fruit factories, there is a strong demand for fruit classification for quality control and packing, which is still manual. To study the application of the proposed gripper with E-skin design in fruit recognition, 6 types of commonly seen fruits (including apple, orange, peach, pear, persimmon, and tangerine) were selected as the grasping objects for the experiment representing automatic sorting for mixed fruits by soft gripper (Fig. 9(a). These 6 fruits are irregular shapes within a similar size range. Since the body of the fruits can be objects with continuity, we adopted the initial E-skin design with a single WEE unit in each arm for this experiment. The grasping for each fruit was repeated 100 times, among which the datasets from 70 times were used for training the MLP model, and the rest were used for testing by random selection. As shown in Fig. 9(b), the recognition accuracy reached 93.89%, which proves that our system and the model can provide reliable classification results for the above-listed fruits through grasping by the soft gripper with E-skin. Our proposed system can potentially be applied to automatic fruit sorting, assembling, and other compatible applications.

V. Conclusion and Future Work

This letter reported a soft robotic gripper integrated with an E-skin based on piezoresistive eutectogel for perception and its application in object recognition through learning. The E-skin unit WEE was designed by packing eutectogel in ecoflex hollow tubes and demonstrated sufficient sensitivity, high stability, and compatibility for facile integration in the soft gripper. The soft gripper could sense deformation information around the E-skin, including its arm bending angle and the contact force from the grasped objects. The multilayer perception model was used to train and test the data acquired by the E-skin through grasping. The recognition accuracy can reach 93.78% for 7 standard objects with 9 geometrical labels and 93.89% for 6 kinds of fruits. The experimental results showed that our proposed E-skin could enable object recognition function in the soft gripper by accessing the size and shape information of the interacting objects. With further sensing optimization and scale adjustment, the industrial soft gripper equipped with our E-skin design has the potential to be applied in automatic fruit/vegetable sorting and assembling if the grasping objects are with similar geometric features to the objects tested in this study.

We also observed varied accuracies among the testing objects. We analyzed the cause in different scenarios, such as data diversity, limited datasets, and array density when interacting with different categories of objects. In the next step, we will focus on 1) optimizing the E-skin design to improve the perception sensitivity, 2) building a large dataset and an advanced model and for learning, 3) developing real-time smart control of the soft gripper based on its perception. We hope this interdisciplinary work can provide new insights into smart interfaces and closed-loop control design in soft robots with a low-cost, green, and facile strategy.

Acknowledgment

The authors would like to thank Prof. Lifeng Yan for his generous support and advice.

References

[1] C. Laschi and M. Cianchetti, "Soft robotics: New perspectives for robot bodyware and control," *Front. Bioeng. Biotechnol.*, vol. 2, Jan. 2014, Art. no. 3.
[2] R. Deimel and O. Brock, "A compliant hand based on a novel pneumatic actuator," in *Proc. IEEE Int. Conf. Robot. Automat.*, 2013, pp. 2047–2053.
[3] C. B. Teeple, T. N. Koutros, M. A. Graule, and R. J. Wood, "Multi-segment soft robotic fingers enable robust precision grasping," *Int. J. Robot. Res.*, vol. 39, no. 14, pp. 1647–1667, 2020.
[4] V. Subramaniam, S. Jain, J. Agarwal, and P. V. y Alvarado, "Design and characterization of a hybrid soft gripper with active palm pose control," *Int. J. Robot. Res.*, vol. 39, no. 14, pp. 1668–1685, 2020.
[5] D. Rus and M. T. Tolley, "Design, fabrication and control of soft robots," *Nature*, vol. 521, no. 7553, pp. 467–475, 2015.
[6] Z. Wang, D. S. Chathuranga, and S. Hirai, "3D printed soft gripper for automatic lunch box packing," in *Proc. IEEE Int. Conf. Robot. Biomimetics*, 2016, pp. 503–508.
[7] J. Zimmer, T. Hellebrekers, T. Asfour, C. Majidi, and O. Kroemer, "Predicting grasp success with a soft sensing skin and shape-memory actuated gripper," in *Proc. IEEE Int. Conf. Intell. Robots Syst.*, 2019, pp. 7120–7127.
[8] A. Nurpeissova, A. Malik, S. Kabitkanov, A. Zhilisbayev, and A. Shintemirov, "An open-source reconfigurable robotic gripper with detachable fingers," in *Proc. IEEE/Amer. Soc. Mech. Engineers 18th Int. Conf. Mechatronic Embedded Syst. Appl., Proc.*, 2022, pp. 1–6.
[9] G. A. Fontanelli et al., "A reconfigurable gripper for robotic autonomous depalletizing in supermarket logistics," *IEEE Robot. Automat. Lett.*, vol. 5, no. 3, pp. 4612–4617, Jul. 2020.
[10] R. J. Webster and B. A. Jones, "Design and kinematic modeling of constant curvature continuum robots: A review," *Int. J. Robot. Res.*, vol. 29, no. 13, pp. 1661–1683, 2010.
[11] M. Yu, W. Liu, J. Zhao, Y. Hou, X. Hong, and H. Zhang, "Modeling and analysis of a composite structure-based soft pneumatic actuators for soft-robotic gripper," *Sensors*, vol. 22, no. 13, 2022, Art. no. 4851.
[12] Y. Hao et al., "A soft bionic gripper with variable effective length," *J. Bionic Eng.*, vol. 15, no. 2, pp. 220–235, 2018.

[13] M. L. Hammock, A. Chortos, B. C. K. Tee, J. B. H. Tok, and Z. Bao, "25th anniversary article: The evolution of electronic skin (E-Skin): A brief history, design considerations, and recent progress," *Adv. Mater.*, vol. 25, no. 42, pp. 5997–6038, 2013.
[14] C. M. Boutry et al., "A hierarchically patterned, bioinspired E-skin able to detect the direction of applied pressure for robotics," *Sci. Robot.*, vol. 3, no. 24, 2018, Art. no. eaau6914.
[15] Q. Hua et al., "Skin-inspired highly stretchable and conformable matrix networks for multifunctional sensing," *Nature Commun.*, vol. 9, no. 1, 2018, Art. no. 244.
[16] W. W. Lee et al., "A neuro-inspired artificial peripheral nervous system for scalable electronic skins," *Sci. Robot.*, vol. 4, no. 32, 2019, Art. no. eaax2198.
[17] S. Sundaram, P. Kellnhofer, Y. Li, J. Y. Zhu, A. Torralba, and W. Matusik, "Learning the signatures of the human grasp using a scalable tactile glove," *Nature*, vol. 569, no. 7758, pp. 698–702, 2019.
[18] T. G. Thuruthel, B. Shih, C. Laschi, and M. T. Tolley, "Soft robot perception using embedded soft sensors and recurrent neural networks," *Sci. Robot.*, vol. 4, no. 26, 2019, Art. no. eaav1488.
[19] B. Shih et al., "Custom soft robotic gripper sensor skins for haptic object visualization," in *Proc. IEEE Int. Conf. Intell. Robots Syst.*, 2017, pp. 494–501.
[20] R. A. Bilodeau, E. L. White, and R. K. Kramer, "Monolithic fabrication of sensors and actuators in a soft robotic gripper," in *Proc. IEEE Int. Conf. Intell. Robots Syst.*, 2015, pp. 2324–2329.
[21] N. Farrow and N. Correll, "A soft pneumatic actuator that can sense grasp and touch," in *Proc. IEEE/RSJ Int. Conf. Intell. Robots Syst.*, 2015, pp. 2317–2323.
[22] D. M. Vogt, Y.-L. Park, and R. J. Wood, "Design and characterization of a soft multi-axis force sensor using embedded microfluidic channels," *IEEE Sensors J.*, vol. 13, no. 10, pp. 4056–4064, Oct. 2013.
[23] Y.-L. Park, B.-R. Chen, and R. J. Wood, "Design and fabrication of soft artificial skin using embedded microchannels and liquid conductors," *IEEE Sensors J.*, vol. 12, no. 8, pp. 2711–2718, Aug. 2012.
[24] H. Zhao, K. O'Brien, S. Li, and R. F. Shepherd, "Optoelectronically innervated soft prosthetic hand via stretchable optical waveguides," *Sci. Robot.*, vol. 1, no. 1, 2016, Art. no. eaai7529.
[25] T. Kim, S. Lee, T. Hong, G. Shin, T. Kim, and Y. L. Park, "Heterogeneous sensing in a multifunctional soft sensor for human-robot interfaces," *Sci. Robot.*, vol. 5, no. 49, 2020, Art. no. eabc6878.
[26] G. Soter, A. Conn, H. Hauser, and J. Rossiter, "Bodily aware soft robots: Integration of proprioceptive and exteroceptive sensors," in *Proc. IEEE Int. Conf. Robot. Automat.*, 2018, pp. 2448–2453.
[27] K. Park, H. Yuk, M. Yang, J. Cho, H. Lee, and J. Kim, "A biomimetic elastomeric robot skin using electrical impedance and acoustic tomography for tactile sensing," *Sci. Robot.*, vol. 7, no. 67, 2022, Art. no. eabm7187.
[28] B. Ying, Q. Wu, J. Li, and X. Liu, "An ambient-stable and stretchable ionic skin with multimodal sensation," *Mater. Horiz.*, vol. 7, no. 2, pp. 477–488, 2020.
[29] H. R. Lee, C. C. Kim, and J. Y. Sun, "Stretchable ionics -A promising candidate for upcoming wearable devices," *Adv. Mater.*, vol. 30, no. 42, 2018, Art. no. 1704403.
[30] B. Ying, R. Z. Chen, R. Zuo, J. Li, and X. Liu, "An anti-freezing, ambient-stable and highly stretchable ionic skin with strong surface adhesion for wearable sensing and soft robotics," *Adv. Funct. Mater.*, vol. 31, no. 42, 2021, Art. no. 2104665.
[31] R. Zuo, Z. Zhou, B. Ying, and X. Liu, "A soft robotic gripper with anti-freezing ionic hydrogel-based sensors for learning-based object recognition," in *Proc. IEEE Int. Conf. Robot. Automat.*, 2021, pp. 12164–12169.
[32] R. Bai, Q. Yang, J. Tang, X. P. Morelle, J. Vlassak, and Z. Suo, "Fatigue fracture of tough hydrogels," *Extreme Mechanics Lett.*, vol. 15, pp. 91–96, 2017.
[33] X. Zheng, Y. Gao, X. Ren, and G. Gao, "Polysaccharide-tackified composite hydrogel for skin-attached sensors," *J. Mater. Chem. C*, vol. 9, no. 9, pp. 3343–3351, 2021.
[34] B. Wu et al., "Interfacial reinitiation of free radicals enables the regeneration of broken polymeric hydrogel actuators," *CCS Chem.*, vol. 5, no. 3, pp. 704–717, 2023.
[35] M. C. Bubalo, K. Radošević, I. R. Redovniković, I. Slivac, and V. G. Srček, "Toxicity mechanisms of ionic liquids," *Arhiv za Higijenu Rada i Toksikologiju*, vol. 68, no. 3, pp. 171–179, 2017.
[36] J. Wang, C. Teng, and L. Yan, "Applications of deep eutectic solvents in the extraction, dissolution, and functional materials of chitin: Research progress and prospects," *Green Chem.*, vol. 24, no. 2, pp. 552–564, 2022.
[37] J. Wang and A. Chortos, "Control strategies for soft robot systems," *Adv. Intell. Syst.*, vol. 4, no. 5, 2022, Art. no. 2100165.
[38] A. Zolfagharian, A. Kaynak, and A. Kouzani, "Closed-loop 4D-printed soft robots," *Mater. Des.*, vol. 188, 2020, Art. no. 108411.
[39] B. Finio, R. Shepherd, and H. Lipson, "Air-powered soft robots for K-12 classrooms," in *Proc. IEEE Innov. Softw. Eng. Conf. 3rd Integr. Sci., Technol., Eng., Math. Educ. Conf.*, 2013, pp. 1–6.
[40] Y. Wu, Y. Deng, K. Zhang, Y. Wang, L. Wang, and L. Yan, "A flexible and highly ion conductive polyzwitterionic eutectogel for quasi-solid state zinc ion batteries with efficient suppression of dendrite growth," *J. Mater. Chem. A*, vol. 10, no. 34, pp. 17721–17729, 2022.

IEEE Robotics and Automation Letters (RA-L) paper, presented at ICRA 2024, Yokohama, Japan. Cite as RA-L paper.